NEUTRINO EMISSION DUE TO ELECTRON BREMSSTRAHLUNG IN SUPERFLUID NEUTRON-STAR CORES

A.D. Kaminker

A.F. Ioffe Physical Technical Institute
194021 St.Petersburg, Russia
e-mail: kam@astro.ioffe.rssi.ru

and P. Haensel

N. Copernicus Astronomical Center, Polish Academy of Sciences
Bartycka 18, 00-716 Warszawa, Poland
e-mail: haensel@camk.edu.pl

(Received January 13, 1999)

We study neutrino energy emission rates (emissivities) due to electron bremsstrahlung produced by *ee* and *ep* collisions in the superfluid neutron star cores. The neutrino emission due to *ee* collisions is shown to be the dominant neutrino reaction at not too high temperatures ($T \lesssim 10^8$ K) in dense matter if all other neutrino reactions involving nucleons are strongly suppressed by neutron and proton superfluidity. Simple practical expressions for the *ee* and *ep* neutrino emissivities are obtained. The efficiency of various neutrino reactions in the superfluid neutron–star cores is discussed for the cases of standard neutrino energy losses and the losses enhanced by the direct Urca process.

PACS numbers: 97.60.Jd, 26.60.+c, 23.40.Bw

1. Introduction

In the first 10^5 years of their life, neutron stars (NSs) cool mainly via neutrino emission from their cores. This emission results from weak interaction processes involving baryons and leptons. It is important, thus, to study various neutrino reactions. For simplicity, we will mainly consider the NS cores composed of neutrons n, with some admixture of protons p and electrons e. The neutrino reactions in the neutron-star cores are traditionally divided into two groups, which differ drastically by their efficiency and produce the *standard* or *rapid* cooling (*e.g.*, Ref. [1]).

The standard cooling is mainly provided by the neutron and proton branches of the modified Urca reactions [2, 3]

$$n + N \to p + N + e + \bar{\nu}_e \ , \qquad p + e + N \to n + N + \nu_e \ , \tag{1}$$

where N is a nucleon (n or p), and by the nucleon–nucleon (nn, np, and pp) bremsstrahlung processes

$$N + N \to N + N + \nu + \bar{\nu} \ . \tag{2}$$

The rapid cooling is strongly enhanced by the direct Urca processes

$$n \to p + e + \bar{\nu}_e \ , \qquad p + e \to n + \nu_e \ , \tag{3}$$

which can operate [4] only in the central regions of rather massive NSs with proton fraction exceeding 11% of the total baryon density. If the direct Urca reaction is allowed (in a non-superfluid NS), the neutrino emissivity is typically 4–5 orders of magnitude higher than in the standard reactions (1) and (2).

It is widely accepted (see, *e.g.*, [5, 6] and references therein), that neutrons and protons in a NS core can be in a superfluid state. The superfluidity is generally thought to be of BCS type, produced by attractive component of nuclear forces. Various microscopic theories predict very different critical temperatures of neutron and proton superfluids, T_{cn} and T_{cp}, which range from 10^8 to 10^{10} K. The neutron superfluidity in the NS cores is generally believed to be produced by triplet-state pairing of neutrons (with anisotropic superfluid energy gap), while the proton superfluidity is due to the singlet-state pairing (with isotropic gap). If $T \ll T_{cn}$ and $T \ll T_{cp}$ the superfluidity strongly suppresses all the neutrino reactions (1)–(3) involving nucleons (*e.g.*, [1, 3, 7]).

Onset of the neutron or proton superfluidity with the decrease of temperature in a cooling NS initiates also an additional specific neutrino reaction which can be considered as neutrino production due to Cooper pairing of quasinucleons $\widetilde{N}$

$$\widetilde{N} + \widetilde{N} \to \nu + \bar{\nu} \ . \tag{4}$$

The emission due to singlet-state pairing of neutrons has been calculated by Flowers *et al.* [8] and Voskresensky & Senatorov [9, 10] while the emission due to triplet-state pairing of neutrons and singlet-state pairing of protons has been determined by Yakovlev *et al.* [11, 12] and Kaminker *et al.* [13]. The effect is much stronger for neutrons than for protons due to the smallness of axial–vector electroweak currents for protons.

In contrast to the non-superfluid cores, where the main neutrino emission is produced either by the modified or by the direct Urca processes (depending on the equation of state and density), very different neutrino mechanisms can dominate in the superfluid cores, depending on the relative magnitudes of T, T_{cn} and T_{cp}. In particular, Cooper-pair neutrino emission (4) can be very important if $0.1\,T_{cN} \lesssim T \lesssim T_{cN}$ (*e.g.*, Ref. [12]). At lower temperatures, $T \ll T_{cN}$, this emission falls exponentially.

On the other hand, as mentioned by Schaab *et al.* [14], an additional neutrino emission mechanism, the neutrino-pair bremsstrahlung due to ep scattering

$$e + p \to e + p + \nu + \bar{\nu} \ , \tag{5}$$

can be important in the superfluid NS cores. This mechanism, and the closely related mechanism of neutrino bremsstrahlung due to ee scattering

$$e + e \to e + e + \nu + \bar{\nu} \tag{6}$$

has been considered briefly by Kaminker *et al.* [15]. The latter authors have estimated the neutrino energy emission rates (emissivities) in these reactions using simplified criteria of similarity of neutrino emission and electron conduction processes. It is quite evident that these reactions, especially the neutrino ee bremsstrahlung, can be important in highly superfluid NS cores, where all the reactions involving nucleons are drastically suppressed by the nucleon superfluidity. Thus, rigorous calculation of the emissivities in the reactions (5) and (6) deserves special study.

Notice that the neutrino bremsstrahlung due to ee scattering of nondegenerate electrons at not too high densities, $\rho \lesssim 10^{10}$ g cm^{-3} (corresponding to the outer NS crust), was considered by Cazzola & Saggion [16, 17]. The authors obtained general but cumbersome expressions for the emissivity [16] and performed numerical calculations using Monte Carlo method [17]. The main result of their consideration was that the emissivity due to the ee bremsstrahlung did not exceed 1% of the total emissivity from other neutrino reactions in a NS crust (pair annihilation, photoneutrino and plasmon decay). We will show that this is not so in a NS core.

The aim of the present article is to carry out an accurate calculation of the neutrino emissivities for the bremsstrahlung reactions (5) and (6), and to analyze the efficiency of various neutrino production mechanisms (1)–(6) in superfluid NS cores.

2. Superfluid neutron-star cores

Mass density of the matter in a NS core is expected to range from about $0.5\rho_0$ at its outer edge [18], to (5–10)ρ_0 at the stellar center, where $\rho_0 = 2.8 \times 10^{14}$ g cm^{-3} is the saturation density of nuclear matter. At $\rho \lesssim 2\rho_0$, neutron-star matter consists mostly of neutrons, with a few percent admixture of protons, electrons, and possibly muons. The fraction of muons is usually much smaller than that of electrons, and a simple *npe* model is a good approximation. At higher densities, $\rho \gtrsim 2\rho_0$, other particles may appear, such as hyperons, condensed pions or kaons, or even free (deconfined) quarks. Neutrino emissivity of dense neutron-star matter with different compositions has been reviewed by Pethick [1]. For simplicity, we will neglect possible presence of hyperons and exotic particles, and consider *npe* matter only. All constituents of the matter are strongly degenerate. The electrons form an ultrarelativistic and almost ideal gas, with the electron Fermi-momentum

$$p_{\mathrm{F}e} = \hbar(3\pi^2 n_e)^{1/3} = 648.6\ (n_e/n_0)^{1/3}\, m_e c\ , \qquad (7)$$

where n_e and m_e are electron number density and mass, respectively, and $n_0 = 0.16$ fm^{-3} is the standard nuclear saturation density. The electron Fermi energy (chemical potential) is $\mu_e \approx p_{\mathrm{F}e}c \approx$ (100–300) MeV. Neutrons and protons are nonrelativistic and form strongly interacting Fermi liquids. The condition of beta-equilibrium implies that the chemical potentials of particles satisfy the equality $\mu_n = \mu_p + \mu_e$. Charge neutrality leads to the equality of proton and electron number densities ($n_p = n_e$) and Fermi momenta ($p_{\mathrm{F}e} = p_{\mathrm{F}p}$). The Fermi energy of neutrons is close to that of electrons, while the Fermi energy of protons is much smaller (typically, 3–30 MeV).

Both nucleon species, n and p, can be in a superfluid state (Sect. 1). Microscopically, the superfluidity leads to the appearance of the energy gap Δ in the nucleon dispersion relation. For a triplet-state neutron superfluid, the gap is anisotropic along the neutron Fermi surface. For a singlet-state pairing of protons the gap is isotropic. The proton gap $\Delta_p = \Delta_p(T)$ depends only on temperature T. In the frame of the BCS theory (which we adopt further on), the proton critical temperature T_{cp} is related to the zero-temperature energy gap $\Delta_p(0)$ by $T_{cp} = \Delta_p(0)/(1.764\, k_{\mathrm{B}})$ [19], where k_{B} is the Boltzmann constant.

Superfluidity of neutrons and protons suppresses the main neutrino generation mechanisms (1)–(3) in the NS core and opens an additional neutrino reaction (4). Strong superfluidity of neutrons and protons ($T_{cn} \gg T$ and $T_{cp} \gg T$) suppresses drastically all neutrino reactions (1)–(5) involving nucleons. Superfluidity of protons affects even the neutrino *ee* bremsstrahlung (6), (not very strongly), by changing screening of *ee* interaction.

The plasma screening momentum q_s in npe matter is given by (*e.g.*, Ref. [20])

$$y_s^2 \equiv \frac{q_s^2}{4p_{\mathrm{F}e}^2} = \frac{e^2}{\pi\hbar c}\left(1 + \frac{m_p^* p_{\mathrm{F}p}}{m_e^* p_{\mathrm{F}e}} D_p\right) , \tag{8}$$

where $m_e^* = \mu_e/c^2$ and m_p^* is an effective proton mass (which determines the proton density of states near the Fermi level and which can differ from the bare mass m_p due to polarization effects in dense matter). The first term in brackets comes from the electron screening, while the second term is due to the proton screening. The latter term contains the function D_p. For nonsuperfluid protons ($T \geq T_{cp}$) one has $D_p = 1$, while for $T < T_{cp}$ the factor D_p describes superfluid reduction of proton screening. Gnedin & Yakovlev [20] fitted numerical values of this factor, calculated for singlet-state proton pairing, by

$$\begin{aligned} D_p \;=\; & \left(0.9443 + \sqrt{(0.0557)^2 + (0.1886y)^2}\right)^{1/2} \\ & \times \exp\left(1.753 - \sqrt{(1.753)^2 + y^2}\right) , \end{aligned} \tag{9}$$

where $y = \Delta_p(T)/(k_{\mathrm{B}}T)$. According to Levenfish & Yakovlev [21] the parameter y at any $T < T_{cp}$ is given by the fitting expression

$$y \;=\; \sqrt{1 - \frac{T}{T_{cp}}}\left(1.456 - 0.157\sqrt{\frac{T_{cp}}{T}} + 1.764\,\frac{T_{cp}}{T}\right) . \tag{10}$$

3. General formalism of neutrino *ep* and *ee* bremsstrahlung

Consider two neutrino bremsstrahlung mechanisms (5) and (6) for strongly degenerate, relativistic electrons and strongly degenerate, nonrelativistic protons. We will treat these processes using the standard perturbation theory of weak interactions. We will use the units in which $c = \hbar = k_{\mathrm{B}} = 1$ and return to ordinary physical units in the final expressions.

The emissivities Q_{ep} and Q_{ee} [erg cm^{-3} s^{-1}] of the processes (5) and (6) can be written as

$$\begin{aligned} Q_{12} \;=\; & \frac{\zeta_{12}}{(2\pi)^{14}} \int \mathrm{d}\boldsymbol{p}_1 \int \mathrm{d}\boldsymbol{p}_2 \int \mathrm{d}\boldsymbol{p}_1' \int \mathrm{d}\boldsymbol{p}_2' \int \mathrm{d}\boldsymbol{k}_\nu \int \mathrm{d}\boldsymbol{k}_\nu' \\ & \times \delta^{(4)}(P_1 + P_2 - P_1' - P_2' - K)\, \omega\, f_1 f_2 (1 - f_1')(1 - f_2')\, W, \end{aligned} \tag{11}$$

where $P_1 = (\varepsilon_1, \boldsymbol{p}_1)$ and $P_2 = (\varepsilon_2, \boldsymbol{p}_2)$ are 4-momenta of two charged particles before scattering, $P_1' = (\varepsilon_1', \boldsymbol{p}_1')$ and $P_2' = (\varepsilon_2', \boldsymbol{p}_2')$ are 4-momenta of the

same particles after scattering. Index 1 labels an electron and index 2 labels either a proton or a second electron; $\zeta_{ep} = 1$, $\zeta_{ee} = 1/2$ (to avoid double counting of the same ee scattering events). The quantities $K_\nu = (\omega_\nu, \boldsymbol{k}_\nu)$ and $K'_\nu = (\omega'_\nu, \boldsymbol{k}'_\nu)$ are 4-momenta of neutrino and antineutrino, respectively, and $K = K_\nu + K'_\nu = (\omega, \boldsymbol{k})$ is 4-momentum of the neutrino pair ($\omega = \omega_\nu + \omega'_\nu$ and $\boldsymbol{k} = \boldsymbol{k}_\nu + \boldsymbol{k}'_\nu$). Furthermore,

$$f_i = \left[1 + \exp\left(\frac{\varepsilon_i - \mu_i}{T}\right)\right]^{-1} \tag{12}$$

is a Fermi-Dirac distribution of a particle before scattering (i=1, 2), and f'_i is the corresponding distribution for a particle after scattering. The δ-function describes 4-momentum conservation. Finally, W is the differential transition rate

$$W = \frac{G_{\rm F}^2}{2} \frac{\sum_{\sigma,\nu} |M_{12}|^2}{(2\omega_\nu)(2\omega'_\nu)(2\varepsilon_1)(2\varepsilon_2)(2\varepsilon'_1)(2\varepsilon'_2)} , \tag{13}$$

where $G_{\rm F} = 1.436 \times 10^{-49}$ erg cm^3 is the Fermi weak interaction constant, and $|M_{12}|^2$ is the squared transition amplitude. Summation is over spin states of charged particles before and after scattering $\sigma = (\sigma_1, \sigma_2, \sigma'_1, \sigma'_2)$ and over the neutrino flavors $\nu = (\nu_e, \nu_\mu, \nu_\tau)$. The neutrino energies are assumed to be much lower than the intermediate boson mass ($\sim$80 GeV). The processes in question are represented by four (ep scattering) or eight (ee scattering) Feynman diagrams. Each diagram includes a neutrino-pair emission four-tail vertex. The amplitudes are

$$M_{ep} = M_A, \quad M_{ee} = M_A - M_B , \tag{14}$$

where

$$\begin{aligned} M_A &= 4\pi e^2 l^\alpha \left[\frac{1}{t_{22} - q_s^2} \left(\bar{u}'_2 \gamma^\beta u_2\right) \left(\bar{u}'_1 L^{(1)}_{\alpha\beta} u_1\right)\right. \\ &\quad \left. + \frac{1}{t_{11} - q_s^2} \left(\bar{u}'_1 \gamma^\beta u_1\right) \left(\bar{u}'_2 L^{(2)}_{\alpha\beta} u_2\right)\right] , \qquad (15) \\ M_B &= 4\pi e^2 l^\alpha \left[\frac{1}{t_{21} - q_s^2} \left(\bar{u}'_1 \gamma^\beta u_2\right) \left(\bar{u}'_2 L^{(3)}_{\alpha\beta} u_1\right)\right. \\ &\quad \left. + \frac{1}{t_{12} - q_s^2} \left(\bar{u}'_2 \gamma^\beta u_1\right) \left(\bar{u}'_1 L^{(4)}_{\alpha\beta} u_2\right)\right] , \qquad (16) \end{aligned}$$

$$\begin{aligned} L^{(1)}_{\alpha\beta} &= \Gamma_{e\alpha}\, G_e(P'_1 + K)\, \gamma_\beta + \gamma_\beta\, G_e(P_1 - K)\, \Gamma_{e\alpha} , \\ L^{(2)}_{\alpha\beta} &= \Gamma_{2\alpha}\, G_2(P'_2 + K)\, \gamma_\beta + \gamma_\beta\, G_2(P_2 - K)\, \Gamma_{2\alpha} , \end{aligned}$$

$$L^{(3)}_{\alpha\beta} = \Gamma_{e\alpha}\, G_e(P_2' + K)\, \gamma_\beta + \gamma_\beta\, G_e(P_1 - K)\, \Gamma_{e\alpha} ,$$
$$L^{(4)}_{\alpha\beta} = \Gamma_{e\alpha}\, G_e(P_1' + K)\, \gamma_\beta + \gamma_\beta\, G_e(P_2 - K)\, \Gamma_{e\alpha} , \qquad (17)$$
$$\Gamma^\alpha_e = C_{eV}\gamma^\alpha + C_{eA}\gamma^\alpha\gamma^5 , \quad \Gamma^\alpha_p = C_{pV}\gamma^\alpha + C_{pA}\gamma^\alpha\gamma^5 , \qquad (18)$$

$l^\alpha = (\bar\psi_\nu \gamma^\alpha (1+\gamma^5)\psi_\nu)$ is neutrino 4-current; u_1, u_1', u_2 and u_2' denote standard bispinor amplitudes of charged particles; ψ_ν and ψ_ν' are the standard bispinor amplitudes of emitted neutrinos; upper bar denotes a Dirac conjugate, Greek indices α and β run over (0,1,2,3), γ^α and γ^5 are Dirac matrices; $G_e(P)$ and $G_p(P)$ are the electron and proton propagators $G_i(P) = (P_\alpha\gamma^\alpha + m_i)/(P^2 - m_i^2)$. We use the bare proton mass $m_2 = m_p$ in the proton propagator and in the normalization of the proton bispinor amplitudes $\bar u_p u_p = 2m_p$ in Eqs. (15) and (17). It will be shown that the final results are independent of m_p which is a consequence of nonrelativistic approximation for protons. Nevertheless the results do depend on the proton density of states near the Fermi level, i.e., on m_p^*. An additional term M_B in M_{ee} appears due to identity of colliding electrons; it contains four diagrams with interchanged final electron states. In Eqs. (15) and (16) we have used photon propagators in the Feynman gauge [22] and four familiar kinematic invariants

$$t_{11} = (P_1 - P_1')^2, \quad t_{22} = (P_2 - P_2')^2,$$
$$t_{21} = (P_2 - P_1')^2, \quad t_{12} = (P_1 - P_2')^2, \qquad (19)$$

where t_{11} and t_{12} are the standard kinematic invariants denoted usually as t and u. We have added the squared screening momentum q_s^2 (see Sect. 2) to the kinematic invariants in the denominators of Eqs. (15) and (16) to account for the plasma screening effects. Furthermore, in Eq. (18) C_{iV} and C_{iA} are, respectively, the vector and the axial vector weak coupling constants associated with four-tail neutrino-emission vertices on electron ($i = e$) or proton ($i = p$) lines of the Feyman diagrams. For emission of $\nu_e\bar\nu_e$ pairs at $i = e$ (charged + neutral currents), one has $C_{eV} = 2\sin^2\theta_{\rm W} + 0.5$ and $C_{eA} = 0.5$, while for emission of $\nu_\mu\bar\nu_\mu$ and $\nu_\tau\bar\nu_\tau$ (neutral currents only), $C'_{eV} = 2\sin^2\theta_{\rm W} - 0.5$ and $C'_{eA} = -0.5$. In this case, $\theta_{\rm W}$ is the Weinberg angle, $\sin^2\theta_{\rm W} \simeq 0.23$. Neutrino emission for $i = p$ goes only via neutral currents and we have $C_{pV} = (1 - 4\sin^2\theta_{\rm W})/2 \approx 0.04$ and $C_{pA} = 1.26/2 = 0.63$, independently of neutrino flavors.

In our case, neutrino-pair momentum is sufficiently small ($k \sim T \ll p_{{\rm F}e}$), so that we can use the approximation of Festa & Ruderman [23] for the electron propagators:

$$G_e(P' + K) = \frac{P'_\alpha\gamma^\alpha}{2(P'K)} , \quad G_e(P - K) = -\frac{P_\alpha\gamma^\alpha}{2(PK)} \qquad (20)$$

and the nonrelativistic approximation for the proton propagators

$$G_{\rm p}(P_2'+K) = -G_{\rm p}(P_2-K) = \frac{1+\gamma^0}{2\omega}\ . \tag{21}$$

The standard tedious calculations using the Lenard identity [22]

$$\begin{aligned}&\int {\rm d}\boldsymbol{k}_\nu \int {\rm d}\boldsymbol{k}'_\nu\, \delta^{(4)}(K-K_\nu-K'_\nu)\,\frac{K_\nu^\alpha K'^\beta_\nu}{\omega_\nu\omega'_\nu}\\ &= \frac{\pi}{6}(K^2 g^{\alpha\beta}+2K^\alpha K^\beta)\ ,\end{aligned} \tag{22}$$

yield

$$\begin{aligned}Q_{12} \ =\ & \frac{e^4\,G_{\rm F}^2}{12(2\pi)^{11}}\,\zeta_{12}\int {\rm d}\boldsymbol{p}_1\int {\rm d}\boldsymbol{p}_2\int {\rm d}\boldsymbol{p}'_1\int {\rm d}\boldsymbol{p}'_2\,\frac{\omega}{\varepsilon_1\varepsilon'_1\varepsilon_2\varepsilon'_2}\\ &\times J_{12}\,f_1 f_2(1-f'_1)(1-f'_2)\,.\end{aligned} \tag{23}$$

For ep scattering we have

$$J_{ep} = \frac{2^6 C_{e+}^2\, m_p^2}{(t_{22}-q_s^2)^2}\,\frac{K^2(P_1P'_1)(2\varepsilon_1\varepsilon'_1-P_1P'_1)}{(P_1K)(P'_1K)}\,, \tag{24}$$

where $C_{e+}^2 = \sum_\nu (C_{eV}^2 + C_{eA}^2)$. Notice that Q_{ep} determined by Eqs. (23) and (24) appears to be very similar to the emissivity $Q_{\rm br}$ given by Eqs. (A7) and (A13) in the article by Haensel *et al.* [24] who considered neutrino bremsstrahlung due to Coulomb scattering of electrons by atomic nuclei in the NS crust. Equation (24) describes only neutrino emission associated with electron lines of the Feynman diagrams and does not include analogous emission associated with proton lines (the second term in Eq. (15)) which vanishes in the limit of nonrelativistic protons.

In the case of ee scattering we have

$$J_{ee} = C_{e+}^2\,K^2(J_1+J_2-J_3)\ , \tag{25}$$

where

$$\begin{aligned}J_1 \ =\ & X_1 - I_1\ ,\quad J_2 = X_2 - I_2\ ,\quad J_3 = Y_1+Y_2+Z_1+Z_2\ ,\\ I_1 \ =\ & \frac{2^6}{(t_{11}-q_s^2)(t_{22}-q_s^2)}\left[(P_1P_2)(P'_1P'_2)+\frac{C_{e-}^2}{C_{e+}^2}(P_1P'_2)(P_2P'_1)\right]\\ & \times\left[\frac{(P'_1P'_2)}{(P'_1K)(P'_2K)}+\frac{(P_1P_2)}{(P_1K)(P_2K)}-\frac{(P_1P'_2)}{(P_1K)(P'_2K)}-\frac{(P_2P'_1)}{(P_2K)(P'_1K)}\right],\\ X_1 \ =\ & 2^6\,\left[(P_1P_2)(P'_1P'_2)+(P_2P'_1)(P_1P'_2)\right]\end{aligned}$$

$$\times \left[\frac{1}{(t_{22}-q_s^2)^2} \, \frac{(P_1P_1')}{(P_1K)(P_1'K)} + \frac{1}{(t_{11}-q_s^2)^2} \, \frac{(P_2P_2')}{(P_2K)(P_2'K)} \right],$$

$$Y_1 = \frac{2^6 (P_1P_2)(P_1'P_2')}{(t_{11}-q_s^2)(t_{12}-q_s^2)} \times \left[\frac{(P_1'P_2')}{(P_1'K)(P_2'K)} - \frac{(P_2P_1')}{(P_2K)(P_1'K)} - \frac{(P_2P_2')}{(P_2K)(P_2'K)} \right],$$

$$Z_1 = \frac{2^6 (P_1P_2)(P_1'P_2')}{(t_{22}-q_s^2)(t_{12}-q_s^2)} \times \left[\frac{(P_1P_2)}{(P_1K)(P_2K)} - \frac{(P_1P_1')}{(P_1K)(P_1'K)} - \frac{(P_2P_1')}{(P_2K)(P_1'K)} \right], \tag{26}$$

where $C_{e-}^2 = \sum_\nu (C_{eV}^2 - C_{eA}^2)$. The expressions for I_2 and X_2 are obtained from those for I_1 and X_1 by replacing $1 \rightleftarrows 2$. The expressions for Y_2 and Z_2 are obtained from those for Y_1 and Z_1 by replacing $1 \rightleftarrows 2$ and $1' \rightleftarrows 2'$ simultaneously. The quantities defined in Eqs. (26) possess numerous symmetry properties. For instance, X_1 is invariant with respect to replacing $1 \rightleftarrows 2$ and $1' \rightleftarrows 2'$, etc. The integrand in (23) can be shown to be highly symmetric as well. Using the symmetry properties one can easily prove that in Eq. (23) it is sufficient to use the expression

$$J_{ee} = 2\, C_{e+}^2 \, K^2 (X - I_1 - Y_1 - Z_1) \; . \tag{27}$$

In this case

$$X = 2^7 \, \frac{(P_1P_2)(P_1'P_2') + (P_2P_1')(P_1P_2')}{(t_{22}-q_s^2)^2} \, \frac{(P_1P_1')}{(P_1K)(P_1'K)} \tag{28}$$

corresponds to "direct" ee scattering, i.e., to square of any single term (amplitude) in M_A or M_B in Eqs. (14)–(16); I_1 corresponds to interference of amplitudes with exchanging electrons 1 and 2 ($1 \rightleftarrows 2, 1' \rightleftarrows 2'$); while Y_1 and Z_1 correspond to interference of amplitudes with mutually transposed electron final states $1' \rightleftarrows 2'$.

For further analysis, it is convenient to introduce an appropriate 4-momentum transfer $Q = P_2' - P_2 = P_1 - P_1' - K = (\Omega, \boldsymbol{q})$ from particle 1 to particle 2 due to Coulomb interaction. Using the 4-momentum conserving delta-function in Eq. (11) we can remove the integration over $\boldsymbol{p}_1'$ and over ω, and then replace the integration over $\boldsymbol{p}_2'$ by the integration over $\boldsymbol{q}$. It is convenient also to express Q_{ep} and Q_{ee} in the form suggested by Haensel *et al.* [24] for the emissivity $Q_{\rm br}$ of the neutrino bremsstrahlung due to scattering of electrons off atomic nuclei in the NS envelopes:

$$Q_{12} = \frac{8\pi G_{\rm F}^2 e^4 C_{e+}^2}{567} \, T^6 n_2 L_{12} \; . \tag{29}$$

In a Coulomb liquid of atomic nuclei, a dimensionless quantity L_{12} has meaning of a Coulomb logarithm. For neutrino ee and ep bremsstrahlung, we are interested in, L_{12} is a dimensionless function to be evaluated. General expressions for L_{12} are

$$L_{ep} = \frac{567}{(2\pi)^{10}T^6 p_{\mathrm{F}p}^3}\int \mathrm{d}\boldsymbol{p}_1\int \mathrm{d}\boldsymbol{p}_2\int \mathrm{d}\boldsymbol{q}\int \mathrm{d}\boldsymbol{k}\ \frac{\omega}{\varepsilon_1\varepsilon_1'} \times\frac{K^2}{(q^2+q_s^2)^2}\frac{(P_1P_1')(2\varepsilon_1\varepsilon_1'-P_1P_1')}{(P_1K)(P_1'K)}f_1f_2(1-f_1')(1-f_2')\ , \quad (30)$$

$$L_{ee} = \frac{567}{2^{16}\pi^{10}T^6 p_{\mathrm{F}e}^3}\int \mathrm{d}\boldsymbol{p}_1\int \mathrm{d}\boldsymbol{p}_2\int \mathrm{d}\boldsymbol{q}\int \mathrm{d}\boldsymbol{k}\ \frac{\omega}{\varepsilon_1\varepsilon_1'\varepsilon_2\varepsilon_2'} \times K^2\,(X-I_1-Y_1-Z_1)\,f_1f_2\,(1-f_1')(1-f_2')\ . \quad (31)$$

To obtain Eq. (30) we set $\varepsilon_2\varepsilon_2' = m_p^2$ in the denominator of (23) because the protons are nonrelativistic.

Since charged particles are strongly degenerate, the main contribution to L_{12} comes from those transitions, in which the particle momenta before and after collisions lie in the narrow thermal shells around their Fermi surfaces, $|\varepsilon-\mu| \lesssim T$. In Eqs. (30) and (31) we may set $\mathrm{d}\boldsymbol{p}_i = m_i^* p_{\mathrm{F}i}\,\mathrm{d}\varepsilon_i\,\mathrm{d}\Omega_i$, where $\mathrm{d}\Omega_i$ is solid angle element in the direction of $\boldsymbol{p}_i$. We also put $\varepsilon_1 = p_1$ in Eqs. (30) and (31), and $\varepsilon_2 = p_2$ in Eq. (31), respectively, since electrons are ultrarelativistic.

Following Haensel *et al.* [24] we introduce the quantities $\boldsymbol{q} = \boldsymbol{q}_t + \boldsymbol{q}_r$, $\boldsymbol{k} = \boldsymbol{k}_t + \boldsymbol{k}_r$ and $\boldsymbol{p}_1'' = \boldsymbol{p}_1 - \boldsymbol{q}_t = \boldsymbol{p}_1' + \boldsymbol{q}_r + \boldsymbol{k}$, where $\boldsymbol{q}_t$ corresponds to purely elastic Coulomb scattering while $\boldsymbol{q}_r$ takes into account inelasticity; vector $\boldsymbol{p}_1''$ is directed along $\boldsymbol{q}_r$ but has the same length as $\boldsymbol{p}_1$, i.e., $|\boldsymbol{p}_1''| = |\boldsymbol{p}_1|$; $\boldsymbol{k}_r$ and $\boldsymbol{k}_t$ are the orthogonal vector components parallel and perpendicular to $\boldsymbol{p}_1''$, respectively. Notice that $q_t = 2p_1\sin(\vartheta/2)$, where ϑ is an angle between $\boldsymbol{p}_1$ and $\boldsymbol{p}_1''$. Strong electron degeneracy implies $q_r \ll p_{\mathrm{F}e}$, $k \ll p_{\mathrm{F}e}$ and $\Omega \ll p_{\mathrm{F}e}$, although q_t can be comparable to $p_{\mathrm{F}e}$ for large-angle electron scattering events. From geometrical consideration and energy-momentum conservation in analogy with expressions given by Haensel *et al.* [24] we obtain

$$\begin{aligned} q^2 &= (\boldsymbol{q}_t+\boldsymbol{q}_r)^2 = q_t^2+q_r^2-q_t^2\,(q_r/p_{\mathrm{F}e})\,,\\ P_1P_1' &\approx (q_t^2+k_t^2+2\boldsymbol{q}_t\cdot\boldsymbol{k})/2\,,\\ P_1K &\approx p_1(q_r-\Omega)-\boldsymbol{q}_t\cdot\boldsymbol{k},\quad P_1'K \approx p_1(q_r-\Omega)\,,\\ \Omega+\omega &= \varepsilon_1-\varepsilon_1' \approx q_r+k_r\ ,\\ K^2 &= \omega^2-k_r^2-k_t^2 \approx k_0^2-k_t^2\,. \end{aligned} \quad (32)$$

Here, $k_0^2 = (q_r - \Omega)(2\omega - q_r + \Omega)$, and the condition $K^2 > 0$ yields $k_0 \geq k_t$ and $q_r \geq \Omega$, $\omega \geq (q_r - \Omega)/2 \geq 0$.

In what follows, we consider *ep* and *ee* scattering separately.

4. Neutrino *ep* bremsstrahlung

Let us evaluate Q_{ep} from Eqs. (29) and (30):

$$L_{ep} = \frac{567 m_p^*}{(2\pi)^{10} T^6} \int \mathrm{d}\varepsilon_1 \int \mathrm{d}\varepsilon_2 \int \mathrm{d}\Omega_1 \int \mathrm{d}\Omega_2 \int\limits_0^{2\pi} \mathrm{d}\varphi_q \int\limits_0^{2p_{\mathrm{F}e}} \mathrm{d}q_t \, q_t$$
$$\times \int\limits_{-\infty}^{\infty} \mathrm{d}q_r \int\limits_{(q_r-\Omega)/2}^{\infty} \mathrm{d}\omega \int\limits_0^{2\pi} \mathrm{d}\varphi \int\limits_0^{k_0} \mathrm{d}k_t \, k_t \, f_1 \, f_2 \, (1 - f_1') \, (1 - f_2')$$
$$\times \frac{\omega}{\varepsilon_1 \varepsilon_1'} \, \frac{(k_0^2 - k_t^2)}{(q_t^2 + q_r^2 - \Omega^2 + q_s^2)^2} \, \frac{q_t^2 \, [1 - q_t^2/(4p_{\mathrm{F}e}^2)]}{(q_r - \Omega)(q_r - \Omega - \boldsymbol{q}_t \cdot \boldsymbol{k}/p_{\mathrm{F}e})} \, , \tag{33}$$

where we have introduced integration over $\mathrm{d}\boldsymbol{q} = \mathrm{d}\varphi_q \, \mathrm{d}q_t \, q_t \, \mathrm{d}q_r$ with cylindrical axis along $\boldsymbol{p}_1$ and integration over $\mathrm{d}\boldsymbol{k} = \mathrm{d}\varphi \, k_t \, \mathrm{d}k_t \, \mathrm{d}\omega$ with cylindrical axis along $\boldsymbol{p}_1''$. In the latter integration we have used the equality $\mathrm{d}k_r = \mathrm{d}\omega$; φ is an azimuthal angle of $\boldsymbol{k}$ with respect to the $\boldsymbol{p}_1''$-axis.

Consider the case of $q_s \ll p_{\mathrm{F}e}$ typical for the NS cores, where q_s is the plasma screening momentum (Sect. 2). Integration in Eq. (33) can be simplified because the main contribution comes from the values $q_s \lesssim q \ll p_{\mathrm{F}e}$ which correspond to the *small-angle approximation*. In this approximation, we can omit $q_t^2/(2p_{\mathrm{F}e})^2$ in the numerator and $\boldsymbol{q}_t \cdot \boldsymbol{k}/p_{\mathrm{F}e}$ in the denominator of the integrand. Furthermore we may set $1/(\varepsilon_1 \varepsilon_1') = 1/p_{\mathrm{F}e}^2$ in the integrand of (33) and take into account that the energy transfer Ω from an electron to a proton is

$$\Omega = \varepsilon_2 - \varepsilon_2' \approx \frac{1}{m_p^*} \left(\boldsymbol{p}_2 \cdot \boldsymbol{q} + \frac{q^2}{2} \right) \approx \frac{p_{\mathrm{F}e} q}{m_p^*} \cos\vartheta_{q2} \, , \tag{34}$$

where ϑ_{q2} is an angle between $\boldsymbol{q}$ and $\boldsymbol{p}_2$. Then the integrand in Eq. (33) depends only on the relative positions of $\boldsymbol{p}_2$ and $\boldsymbol{q}$.

First we can fix positions of $\boldsymbol{p}_1$, $\boldsymbol{p}_2$ and $\boldsymbol{q}$ and perform the following integrations:

$$\int\limits_0^{2\pi} \mathrm{d}\varphi \int\limits_0^{k_0} \mathrm{d}k_t \, k_t (k_0^2 - k_t^2) = 2\pi (q_r - \Omega)^2 \left[\omega - \frac{1}{2}(q_r - \Omega) \right]^2 \, . \tag{35}$$

A sequence of angular integrations yields $\int \mathrm{d}\Omega_1 \int \mathrm{d}\varphi_q \int \mathrm{d}\Omega_2 \ldots = 16\pi^3 \int \mathrm{d}\cos\vartheta_{q2} \ldots$ Finally, we are left with the only angular integration in Eq. (33) , that over $\mathrm{d}\cos\vartheta_{q2}$. According to Eq. (34), the variation range of $\cos\vartheta_{q2}$ is related to variation range of Ω. Let us consider two extreme cases.

Low temperature limit ($T \ll q_s p_{\mathrm{F}e}/m_p^* \ll q_s$) corresponds to thermal energies T much less than recoil energy of protons. This case is most important for practical use [15]. Let us replace integration over $\cos\vartheta_{q2}$ by integration over Ω: $\cos\vartheta_{q2} = m_p^*\Omega/(q_t p_{\mathrm{F}e})$, where $(q_r - 2\omega) \le \Omega \le q_r$. The Pauli principle strongly restricts possible values of Ω as well as final states of electrons and protons.

The condition $T \ll q_s$ leads to the inequalities $q_r \ll q_t$, $\omega \ll q_t$, $\Omega \ll q_t$. The integration over $\mathrm{d}q_t$ in Eq. (33) yields

$$\int_0^{2p_{\mathrm{F}e}} \mathrm{d}q_t \, \frac{q_t^2}{(q_t^2 + q_s^2)^2} \simeq \frac{1}{2p_{\mathrm{F}e}} \left(\frac{\pi}{4y_s} - 1 \right) , \tag{36}$$

where y_s is given by Eq. (8).

The integrations over ε_1 and ε_2 are standard:

$$\begin{aligned} &\int_{-\infty}^{+\infty} \mathrm{d}\varepsilon_1 \int_{-\infty}^{+\infty} \mathrm{d}\varepsilon_2 \; f_1 f_2 \, (1 - f_1') \, (1 - f_2') \\ &= \frac{(\omega + \Omega)}{\mathrm{e}^{(\omega+\Omega)/T} - 1} \, \frac{\Omega}{1 - \mathrm{e}^{-\Omega/T}} \quad \text{for } \Omega > 0 \, , \, (\omega + \Omega) > 0; \\ &= \frac{(|\Omega| - \omega)}{1 - \mathrm{e}^{-(|\Omega|-\omega)/T}} \, \frac{|\Omega|}{\mathrm{e}^{|\Omega|/T} - 1} \quad \text{for } \Omega < 0, \, (\omega + \Omega) < 0, \end{aligned} \tag{37}$$

where $\varepsilon_1' = \varepsilon_1 - \omega - \Omega$ and $\varepsilon_2' = \varepsilon_2 + \Omega$. Now we are left with integrations over $\mathrm{d}\omega \, \mathrm{d}\Omega \, \mathrm{d}q_r$ in six domains restricted by the inequalities $q_r \ge \Omega$ and $\omega \ge (q_r - \Omega)/2 \ge 0$ (see Eqs. (32)). Three of them correspond to $q_r > 0$ [(a) $\Omega \ge 0$; (b) $\Omega < 0$, $\omega + \Omega \ge 0$; (c) $\omega + \Omega < 0$], while three others correspond to $0 \ge q_r \ge \Omega$ [(d) $\omega + \Omega \ge 0$; (e) $2\omega + \Omega \ge 0 > \omega + \Omega$; (f) $0 > 2\omega + \Omega \ge q_r$]. Following Haensel *et al.* [24] we can introduce dimensionless variables $u = q_r/T$, $w = \Omega/T$, $v = \omega/T$, $v_0 = (q_r - \Omega)/(2T)$. Six domains of integration over $\mathrm{d}v \, \mathrm{d}w \, \mathrm{d}v_0$ in Eq. (33) are reduced to four ones, and integration over $\mathrm{d}v_0$ is trivial ($\int_0^v \mathrm{d}v_0 \, (v - v_0)^2 = v^3/3$).

Finally, using Eqs. (33), (35), (36), and (37) we obtain

$$L_{ep} \approx \frac{189 m_p^{*2} T^2}{2^7 \pi^5 p_{\mathrm{F}e}^4 y_s} \eta = \frac{3\pi^3}{40 y_s} \left(\frac{m_p^* T}{p_{\mathrm{F}e}^2} \right)^2 \xi \, , \tag{38}$$

where

$$\eta = \int_0^\infty \mathrm{d}v\, v^4 \left\{ \int_0^\infty \mathrm{d}w\, \frac{w\,(v+w)}{(\mathrm{e}^{v+w}-1)(1-\mathrm{e}^{-w})} + \int_0^v \mathrm{d}w\, \frac{w\,(v+w)}{(\mathrm{e}^{v+w}-1)(1-\mathrm{e}^{-w})} + \int_0^v \mathrm{d}w\, \frac{w\,(v-w)}{(\mathrm{e}^{v-w}-1)(\mathrm{e}^{w}-1)} + \int_{2v}^\infty \mathrm{d}w\, \frac{w\,(v-w)}{(1-\mathrm{e}^{v-w})(\mathrm{e}^{w}-1)} \right\} \approx 1646.7\,, \tag{39}$$

as obtained by numerical integration, and $\xi = 315\,\eta/(16\pi^8) \approx 3.417$.

Kaminker *et al.* [15] proposed to estimate L_{ep} by rescaling the Coulomb logarithm $L_{\rm br}$ calculated by Haensel *et al.* [24] for scattering of ultrarelativistic degenerate electrons by atomic nuclei in liquid state. In the context of *ep* scattering, $L_{\rm br}$ is valid at $T_{{\rm F}p} \ll T \ll T_{{\rm F}e}$. The rescaling procedure has been based on the similarity criterion: $L_{ep} = L_{\rm br}\,\nu_{ep}/\nu_{ep}^{(0)}$, where ν_{ep} is an effective *ep* collision frequency for the conditions under consideration ($T \ll q_s \lesssim T_{{\rm F}p} \ll T_{{\rm F}e}$) and $\nu_{ep}^{(0)}$ is an effective frequency of elastic *ep* collisions at $T \gg q_s$ (*e.g.*, [25]). For $T \ll q_s$, the authors used the collision frequency ν_{ep} that determines the electron thermal conductivity (*e.g.*, [20]). One can easily verify that the result given by Eqs. (38) and (39) differs from the crude estimate by Kaminker *et al.* [15] by a small factor y_s^2 given by (8). Thus Kaminker *et al.* [15] have strongly (typically, by two orders of magnitude) overestimated Q_{ep}, obtained in the present paper by an accurate evaluation. The nature of this overestimation comes from using the effective thermal-conduction collision frequency ν_{ep} in the rescaling procedure. The thermal conduction at $T \ll q_s$ is associated with small momentum transfers ($q \sim T$). Corresponding collision frequency appears to be greatly enhanced as compared to the frequency of collisions with higher momentum transfers ($q \sim q_s$) which should have been used in rescaling. For instance, it would be appropriate to use the *ep* collision frequency which determines electron electric conductivity (*e.g.*, [26]). Therefore, the rescaling proposed in Ref. [15] is basically correct if one uses physically justified effective collision frequencies.

Finally, we obtain (in the standard physical units)

$$Q_{ep} = \frac{\pi^4 \xi\, G_{\rm F}^2 e^4 C_{e+}^2 m_p^{*2}}{945\,\hbar^9 c^8\, y_s\, p_{{\rm F}e}^4}\, n_p\, (k_{\rm B}T)^8 R_{ep} \approx \frac{3.69\times 10^{14}}{y_s} \left(\frac{m_p^*}{m_p}\right)^2 \left(\frac{n_0}{n_p}\right)^{1/3} R_{ep}\, T_9^8 \ \ \mathrm{erg\ cm^{-3}\ s^{-1}}\,. \tag{40}$$

Here we have introduced the factor R_{ep} that describes suppression of the emissivity by the proton superfluidity. We introduced also $T_9 \equiv T/10^9$ K.

If protons are normal ($T \geq T_{cp}$), one has $R_{ep} = 1$ in Eq. (40). The factor R_{ep} reduces neutrino emission at $T < T_{cp}$. It should be the same as the factor R_{np} that describes reduction of the bremsstrahlung neutrino emission in np collisions by proton superfluidity [3]:

$$\begin{aligned} R_{ep} &= \frac{1}{2.732}\left[A\exp\left(1.306-\sqrt{(1.306)^2+y^2}\right)\right. \\ &\quad \left. +\,1.732\,B^7\exp\left(3.303-\sqrt{(3.303)^2+4y^2}\right)\right], \\ A &= 0.9982+\sqrt{(0.0018)^2+(0.3815y)^2}\,, \\ B &= 0.3949+\sqrt{(0.6051)^2+(0.2666y)^2}\,, \end{aligned} \tag{41}$$

where $y = \Delta/T$ (Sect. 2).

Moderate temperature limit ($q_s p_{\mathrm{F}e}/m_p^* \ll T \ll q_s$). In this case thermal energy is much higher than the recoil energy of protons. Therefore, as follows from Eq. (34), $T \gg \Omega$. To estimate L_{ep} in this limit we can omit Ω in comparison with all quantities $\sim T$ in the integrand and in the integration limits in Eq. (33). Note that the condition $k_0^2 \approx q_r(2\omega - q_r) \geq 0$ obviously gives $q_r \geq 0$ and $\omega \geq q_r/2$. Then we easily perform integrations in Eq. (35) and subsequent integrations over $\mathrm{d}\Omega_2\ \mathrm{d}\varphi_q$ and $\mathrm{d}\Omega_1$. In the limit of $\Omega \to 0$ standard integration yields

$$\int \mathrm{d}\varepsilon_1 \int \mathrm{d}\varepsilon_2\ f_1\, f_2\, (1-f_1')\,(1-f_2') \;=\; \frac{\omega\, T}{\mathrm{e}^{\omega/T}-1} \tag{42}$$

which gives

$$\begin{aligned} L_{ep} &= \frac{567 m_p^* T}{2^4\pi^6 p_{\mathrm{F}e}^2}\int\limits_0^{2p_{\mathrm{F}e}} \mathrm{d}q_t\ \frac{q_t^3}{(q_t^2+q_s^2)^2}\int\limits_0^{\infty}\mathrm{d}u\int\limits_{u/2}^{\infty}\mathrm{d}v\,\frac{v^2(v-u/2)^2}{\mathrm{e}^v-1} \\ &= 3\left(\frac{m_p^* T}{p_{\mathrm{F}e}^2}\right) L_{ep}^{(0)}, \\ L_{ep}^{(0)} &= \int\limits_0^{2p_{\mathrm{F}e}} \mathrm{d}q_t\,\frac{q_t^3}{(q_t^2+q_s^2)^2} \;\approx\; \ln\left(\frac{1}{y_s}\right)-\frac{1}{2}\,. \end{aligned} \tag{43}$$

Here $L_{ep}^{(0)}$ is close to the Coulomb logarithm for neutrino bremsstrahlung due to collisions of electrons with nondegenerate protons in the low–temperature limit ($T_{\mathrm{F}p} \lesssim T \ll q_s \ll T_{\mathrm{F}e}$). The factor $3m_p^* T/p_{\mathrm{F}p}^2$ in Eq. (43) appears due

to degeneracy of protons in the case considered here. As a result, we obtain the emissivity (in the standard physical units)

$$Q_{ep} = \frac{8\pi G_{\rm F}^2 e^4 C_{e+}^2 m_p^*}{189\hbar^9 c^8 p_{{\rm F}e}^2} n_p (k_{\rm B}T)^7 L_{ep}^{(0)} R_{ep}$$

$$\approx 1.89 \times 10^{17} \left(\frac{m_p^*}{m_p}\right) \left(\frac{n_p}{n_0}\right)^{1/3} L_{ep}^{(0)} R_{ep} T_9^7 \ \ {\rm erg\ cm^{-3}\ s^{-1}}. \quad (44)$$

Note that at *low temperatures* Q_{ep} has the temperature dependence $Q_{ep} \propto T^8$, which differs from the case of *moderate temperatures*, $Q_{ep} \propto T^7$, as well as from the case of nondegenerate protons, $Q_{ep} \propto T^6$ ($T \gtrsim T_{{\rm F}p}$).

The case $q_s \ll T \lesssim T_{{\rm F}p}$ has no importance for astrophysical applications. It can be shown that in this case the emissivity is again given by Eq. (44) with somewhat different (temperature dependent) Coulomb logarithm $L_{ep}^{(0)}$.

5. Neutrino *ee* bremsstrahlung

Let us consider now the neutrino emissivity Q_{ee} for *ee* bremsstrahlung. We restrict ourselves by the same condition $q_s \ll p_{{\rm F}e}$ (small–angle approximation) as for *ep* bremsstrahlung. In contrast to the previous case, only the region of relatively small temperatures, $T \ll q_s$, is important for practical applications.

The integrand in Eq. (31) depends on the relative positions of $\boldsymbol{p}_1$, $\boldsymbol{p}_2$, $\boldsymbol{q}$ and $\boldsymbol{k}$. In particular it depends on angle Θ between $\boldsymbol{p}_1$ and $\boldsymbol{p}_2$. Thus we may direct $\boldsymbol{p}_1$ along the z-axis and place $\boldsymbol{p}_2$ in the (xz)-plane. Let $(\vartheta_{q1}, \varphi_q)$ be polar angles of $\boldsymbol{q}$ and $(\vartheta_{k1}, \varphi_k)$ be polar angles of $\boldsymbol{k}$. Let us introduce also an angle ϑ_{q2} between $\boldsymbol{q}$ and $\boldsymbol{p}_2$, an angle ϑ_{k2} between $\boldsymbol{k}$ and $\boldsymbol{p}_2$, and a relative azimuthal angle φ_{kq} between $\boldsymbol{k}$ and $\boldsymbol{q}$.

We can use relations (32) as for *ep* bremsstrahlung. While evaluating the right hand side of Eq. (31) it is useful to introduce also an additional auxiliary integral $\int {\rm d}\Omega\, \delta(\varepsilon_2 - \varepsilon_2' + \Omega)$. Using the relation $\varepsilon_2' = |\boldsymbol{p}_2 + \boldsymbol{q}| \approx p_2(1 + (q/p_{{\rm F}e}) \cos\vartheta_{q2})$ we can present the δ–function under this integral in the form

$$\delta(\varepsilon_2 - \varepsilon_2' + \Omega) \approx \frac{1}{q}\, \delta\left(\cos\vartheta_{q2} - \frac{\Omega}{q}\right). \quad (45)$$

Equations (31), (26), (28), (32), and (45) yield

$$L_{ee} = L_{ee}^{(1)} - L_{ee}^{(2)} \approx \frac{567}{2^9\pi^{10}T^6 p_{\mathrm{F}e}} \int \mathrm{d}\varepsilon_1 \int \mathrm{d}\varepsilon_2 \int \mathrm{d}\Omega_1 \int \mathrm{d}\Omega_2 \int_0^{2\pi} \mathrm{d}\varphi_q$$
$$\times \int_0^{2p_{\mathrm{F}e}} \mathrm{d}q_t\, q_t \int_0^{\infty} \mathrm{d}q_r \int_{-\infty}^{q_r} \mathrm{d}\Omega \int_0^{2\pi} \mathrm{d}\varphi \int_{(q_r-\Omega)/2}^{\infty} \mathrm{d}\omega \int_0^{k_0} \mathrm{d}k_t\, k_t$$
$$\times \frac{1}{q}\,\delta\left(\cos\vartheta_{q2} - \frac{\Omega}{q}\right) \frac{(1-\cos\Theta)^2}{(q_t^2+q_r^2-\Omega^2+q_s^2)^2} \frac{(k_0^2-k_t^2)q_t^2}{(q_r-\Omega)^2}$$
$$\times \left[1 - \frac{1+(C_{e-}/C_{e+})^2}{2} \frac{(q_r-\Omega)}{\omega - k\cos\vartheta_{k2}}\right] \omega f_1 f_2 (1-f_1')(1-f_2')\,. \tag{46}$$

Here we have introduced the same notations as in Eq. (33), and we have divided L_{ee} into two parts, $L_{ee}^{(1)}$ and $L_{ee}^{(2)}$. The first part, $L_{ee}^{(1)}$, corresponds to the first term (equal to 1) in square brackets which comes from X in Eq. (31) ("direct" ee scattering). The second part, $L_{ee}^{(2)}$, corresponds to the second term which comes from I_1 in Eq. (31) (interference of amplitudes with exchanging electrons 1 and 2). It can be shown that the terms Y_1 and Z_1 in Eq. (31) (interference of amplitudes with mutually transposed electron final states) contain small parameters $\sim q_r/p_{\mathrm{F}e}$ and $\sim (q_t/p_{\mathrm{F}e})^2$ and can be neglected.

Let us use the relationship $\cos\vartheta_{q2} = \cos\Theta\cos\vartheta_{q1} + \sin\Theta\sin\vartheta_{q1}\cos\varphi_q$ in Eq. (45) and express $\cos\vartheta_{q2}$ in the δ-function through integration variables q_t, q_r, φ_q, and Θ in Eq. (46). We also need to express $\cos\vartheta_{k2}$ through k_r, k_t, φ, and Θ. For this purpose we take into account additional approximate relations (justified at $p_{\mathrm{F}e} \gg q_t$)

$$\cos\vartheta_{q2} \approx (q_r\cos\Theta + q_t\sin\Theta\cos\varphi_q)/q\,,$$
$$\cos\vartheta_{k2} \approx (k_r\cos\Theta + k_t\sin\Theta\cos\varphi_k)/k\,,$$
$$\cos\varphi_k \approx \sin\varphi_{kq} \approx \sin\varphi\,. \tag{47}$$

The third relationship is valid at $q_r \ll q_s \lesssim q_t$, $\Omega \ll q_t$, and $\omega \ll q_t$. First we evaluate $L_{ee}^{(1)}$ in Eq. (46). The integration over $\mathrm{d}\varphi$ is trivial, the integration over k_t is reduced to (35), and the integration over $\mathrm{d}\varphi_q$ can be done with help of the delta-function

$$\delta\left(\cos\vartheta_{q2} - \frac{\Omega}{q}\right) = \frac{q}{q_t\sin\Theta}\,\delta\left(\cos\varphi_q - \frac{\Omega - q_r\cos\Theta}{q_t\sin\Theta}\right)\,. \tag{48}$$

Now we can integrate over $\mathrm{d}\Omega_1$ and $\mathrm{d}\Omega_2$ in a straightforward manner:

$$\int\limits_{4\pi}\int\limits_{4\pi} \mathrm{d}\Omega_1 \mathrm{d}\Omega_2\,(1-\cos\Theta)^2(\sin\Theta)^{-1} = 12\pi^3. \tag{49}$$

The integrations over $\mathrm{d}\varepsilon_1$ and $\mathrm{d}\varepsilon_2$ can be performed using Eq. (37). We are left with a 4-dimensional integral (over $\mathrm{d}\omega\ \mathrm{d}\Omega\ \mathrm{d}q_r\ \mathrm{d}q_t$). Using Eq. (36) and introducing the same dimensionless variables as in Eqs. (38) and (39), we obtain

$$L_{ee}^{(1)} \approx \frac{567\,T^2}{2^8\pi^5\,p_{\mathrm{F}e}^2\,y_s}\;\eta \;=\; \frac{3\pi^3}{16\,y_s}\left(\frac{T}{p_{\mathrm{F}e}}\right)^2\;\xi_1\;, \tag{50}$$

where η is defined by Eq. (39) and $\xi_1 = 189\eta/(16\pi^8) = 2.05$.

Making use of Eqs. (47) and performing straightforward but tedious calculations we can also evaluate $L_{ee}^{(2)}$. It appears to contain a small numerical factor ≈ 0.05 as compared to $L_{ee}^{(1)}$. Note that we have neglected other interference terms in Eq. (31) which could be of the same order of magnitude or even larger than $L_{ee}^{(2)}$. Therefore we will use only the main term (50) for applications.

Finally the neutrino emissivity Q_{ee} can be written in the form (in the standard units)

$$\begin{aligned} Q_{ee} \;&=\; \frac{\pi^4\xi_1 G_{\mathrm{F}}^2 e^4 C_{e+}^2}{378\hbar^9 c^{10} y_s p_{\mathrm{F}e}^2}\, n_e\,(k_{\mathrm{B}}T)^8 \\ &\approx\; \frac{0.69\times 10^{14}}{y_s}\left(\frac{n_e}{n_0}\right)^{1/3} T_9^8 \;\;\mathrm{erg\ cm^{-3}\ s^{-1}}. \end{aligned} \tag{51}$$

As in the case of Q_{ep}, this result differs from a crude estimate given by Kaminker *et al.* [15] by a small factor $y_s^2 \ll 1$ due to an unfortunate use of inappropriate thermal-conduction ee collision frequency in the rescaling procedure.

Let us emphasize that the emissivity Q_{ep} is reduced exponentially by strong proton superfluidity, while Q_{ee} is affected by the superfluidity in a much weaker manner, only through the plasma screening parameter (8). If protons are normal, they provide the major contribution into the plasma screening. If they are strongly superfluid, a weaker electron screening becomes important, which *enhances* Q_{ee}, but not to a great extent (see below).

Let us remind that the neutrino emissivity Q_{ee} for nondegenerate electrons in the neutron star crusts has been calculated by Cazzola & Sagion [16, 17]. We have compared their numerical results (Fig. 2 in Ref. [17]) with our Eq. (51) for several temperatures ($T_9 = 5, 7, 8, 10$) at those values of

$\rho \gtrsim 10^8$ g cm^{-3}, where the relativistic electrons start to become degenerate and both approaches are expected to be qualitatively valid. We have obtained reasonable agreement of the results.

Finally let us make a few remarks about neutrino bremsstrahlung reactions involving muons, μ^-. Muons can appear in sufficiently dense matter of neutron star cores, provided the electron number density exceeds the threshold value $n_e > (m_\mu c)^3/(3\pi^2\hbar^3) = 0.0052$ fm^{-3}, where m_μ is the muon mass. For realistic equations of state, this happens at $\rho \gtrsim$ (1.5–2) ρ_0. The muons, like electrons, form almost ideal degenerate gas, but they are mainly nonrelativistic (near the threshold density) or mildly relativistic at much higher densities. Beta-equilibrium condition implies $\mu_\mu = \mu_e$, where μ_μ is the muon chemical potential. The number density of muons is much smaller than the number density of neutrons or electrons for all densities. In muonic matter, several new neutrino bremsstrahlung reactions are allowed, resulting from μe, $\mu\mu$, μp scattering. The neutrino emissivities in these reactions can be evaluated in the same manner as the emissivities due to ep and ee neutrino bremsstrahlung.

For instance, in the nonrelativistic limit ($p_{\mathrm{F}\mu} \ll m_\mu c$) at $T \ll q_s$, in analogy with Eq. (40), we obtain

$$\begin{aligned} Q_{e\mu} &= \frac{\pi^4 \xi\, G_{\mathrm{F}}^2 e^4 C_{e+}^2 m_\mu^2}{945\hbar^9 c^8 y_s p_{\mathrm{F}\mu}^3 p_{\mathrm{F}e}}\, n_\mu (k_{\mathrm{B}}T)^8 \\ &\approx \frac{4.68\times 10^{12}}{y_s}\left(\frac{n_0}{n_e}\right)^{1/3} T_9^8 \quad \text{erg cm}^{-3}\ \text{s}^{-1}\ , \end{aligned} \tag{52}$$

where n_μ is the muon number density. Equation (52) differs from Eq. (40) by a small factor $(m_\mu/m_p^*)^2$.

One can see that, under considered conditions, the neutrino emissivity $Q_{e\mu}$ is much smaller than the emissivity Q_{ee} due to ee scattering (*cf.* Eqs. (52) and (51)).

Our estimates show that the neutrino bremsstrahlung reactions involving muons are less efficient than analogous reactions involving electrons, for all densities typical for neutron star cores.

6. Discussion

Let us discuss the efficiency of various neutrino emission mechanisms in superfluid NS cores. For illustration, we adopt a moderately stiff equation of state proposed by Prakash *et al.* [27] (the version with compression modulus $K_0 = 180$ MeV and with the same simplified symmetry energy S_V which was used by Page & Applegate [28]). We assume that dense neutron-star

matter consists of neutrons, protons and electrons (no muons and hyperons). The nucleon effective masses will be set equal to 0.7 of the masses of bare particles. The equation of state allows the direct Urca process to operate at $\rho \geq 4.64\,\rho_0$. We consider two densities, $\rho = 2\,\rho_0$, as an example of the standard neutrino cooling (the direct Urca is forbidden), and $\rho = 5\,\rho_0$, representing the case of the cooling enhanced by the direct Urca process. Both nucleon species, neutrons and protons, are supposed to form superfluids. We consider a triplet-state neutron pairing ($^3P_2$), with zero projection of the total momentum ($m_J = 0$) of a Cooper pair onto quantization axis, and a singlet-state proton pairing ($^1S_0$). Since the critical temperatures T_{cn} and T_{cp} of both superfluids, as calculated from microscopic theories, are very model dependent (*e.g.*, Refs. [5, 6, 29-32]), we do not make any specific choice of microscopic superfluid model but treat T_{cn} and T_{cp} as free parameters.

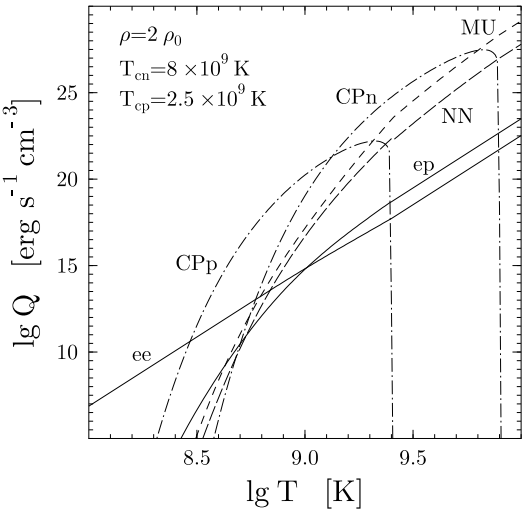

Fig. 1. Temperature dependence of neutrino energy emission rates for various neutrino reactions in *npe* matter at $\rho = 2\,\rho_0$, $T_{cn} = 8 \times 10^9$ K and $T_{cp} = 2.5 \times 10^9$ K. The neutrino reactions are: modified Urca (MU, sum of n and p branches), nucleon-nucleon bremsstrahlung (NN, sum of nn, np and pp branches), ee and ep bremsstrahlung, Cooper pairing of neutrons (CPn) and protons (CPp).

Figures 1 and 2 show temperature dependence of the neutrino emissivities for various neutrino production mechanisms at $\rho = 2\rho_0$ and $\rho = 5\rho_0$, respectively, assuming rather strong neutron and moderate proton superfluids, $T_{cn} = 8 \times 10^9$ K and $T_{cp} = 2.5 \times 10^9$ K.

In Fig. 1 we show neutrino emission from the modified Urca process (1) (sum of the proton and neutron branches), nucleon-nucleon bremsstrahlung

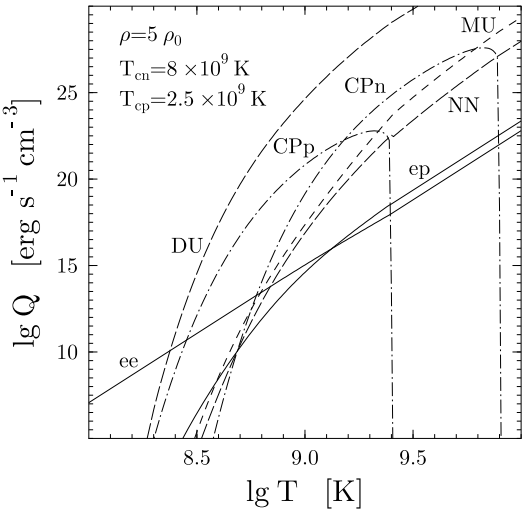

Fig. 2. Same as in Fig. 1 but for $\rho = 5\,\rho_0$. Direct Urca (DU) process is operative, in addition to neutrino reactions shown in Fig. 1.

(2) (sum of *nn*, *np* and *pp* reactions), Cooper pairing of neutrons and protons (4), and *ep* and *ee* bremsstrahlung processes (5) and (6). The emissivities in the last two reactions are obtained in Sects. 4 and 5. The emissivities of the modified Urca and nucleon-nucleon bremsstrahlung reactions (1) and (2) are taken as from Levenfish & Yakovlev [7], with proper account for suppression of the reactions by the neutron and proton superfluidities [3]. The neutrino energy emission rate due to pairing of neutrons is plotted in accordance with the results by Yakovlev *et al.* [11, 12]. The neutrino emission due to pairing of protons is calculated taking into account the relativistic corrections [13] to the non-relativistic result [11, 12]. The allowance for the relativistic corrections increases production of neutrinos due to proton pairing by more than one order of magnitude. The neutrino emissivity due to *ep* bremsstrahlung is calculated in the *low temperature limit* (see Sect. 4) from Eqs. (40) and (41). We use Eq. (51) to obtain the neutrino emission due to *ee* bremsstrahlung.

At $T > T_{cn}$ the neutron-star matter is nonsuperfluid, so that the modified Urca process and nucleon-nucleon bremsstrahlung play leading roles. It can be seen that the nucleon superfluidity reduces the Urca and bremsstrahlung neutrino reactions involving nucleons ((1), (2), and (5)) at $T \lesssim 10^9$ K. On the other hand, the nucleon superfluidity produces two bumps of the partial neutrino emissivities at temperatures slightly below two critical temperatures, T_{cn} and T_{cp}, due to Cooper pairing of neutrons and protons, respectively. The emission due to pairing of neutrons dominates over other

mechanisms at $T \lesssim 6 \times 10^9$ K, while the emission due to pairing of protons dominates at $T \lesssim 1.5 \times 10^9$ K. If the Cooper pairing emission were absent, the total neutrino emissivity at $T \lesssim 10^9$ K would be 2–4 orders of magnitude smaller due to strong suppression by the nucleon superfluidity. The Cooper pairing can easily turn suppression into enhancement at not too low temperatures [11]. However, the Cooper-pairing neutrino reactions are eventually suppressed by superfluidity, when temperature falls down much below the critical temperature of neutrons or protons ($T \lesssim 0.2\,T_{\mathrm{c}N}$). For $T \gtrsim 10^9$ K, the neutrino emission due to *ep* bremsstrahlung turns out to be more intense than that due to *ee* bremsstrahlung but both processes are much weaker than the other neutrino processes. With decreasing T, the situation becomes drastically different. At $T \lesssim 2.5 \times 10^8$ K, *ee* bremsstrahlung becomes the leading mechanism of neutrino emission since it is the only mechanism which is almost insensitive to the superfluid state of matter and suffers no exponential suppression. Let us emphasize that its role is even more important for stronger superfluidities (for higher $T_{\mathrm{c}n}$ and $T_{\mathrm{c}p}$).

In Fig. 2 we plot the contributions from the same neutrino reactions as in Fig. 1 and add the emissivity produced by the powerful direct Urca process (3). The reaction (3) is treated as described by Levenfish & Yakovlev [7], suppressed by nucleon superfluidity as in [21]. The direct Urca process is seen to dominate all other reactions at $T \gtrsim 2 \times 10^8$ K. However, in spite of its high efficiency in nonsuperfluid matter, it is strongly suppressed at low T by nucleon superfluidity, so that *ee* bremsstrahlung becomes the leading neutrino emission mechanism at $T \lesssim 2 \times 10^8$ K. Therefore *ee* bremsstrahlung can play leading role even in the case of neutrino cooling in which the direct Urca process is open (by momentum conservation rules) but strongly reduced by superfluidity. Since the superfluidity reduces the direct Urca emissivity, it reduces also strong difference between the standard and enhanced cooling. The temperature range of the *ee* bremsstrahlung domination is narrower for rapid cooling.

Figures 3 and 4 display the domains of $T_{\mathrm{c}n}$ and $T_{\mathrm{c}p}$, where different neutrino production mechanisms dominate at $T = 2 \times 10^8$ K for the standard and rapid cooling, respectively. Dashes show the lines $T = T_{\mathrm{c}n}$ and $T = T_{\mathrm{c}p}$. In the left lower squares restricted by these lines, neutron-star matter is nonsuperfluid. Accordingly, the modified Urca process in Fig. 3 and the direct Urca process in Fig. 4 are the most powerful neutrino reactions in these domains. In the regions to the right of these domains neutrons are superfluid but protons are not, while in the regions above these domains protons are superfluid and neutrons are not. In the upper right squares enclosed by the dashed lines both nucleon species, n and p, are superfluid. One can see a variety of dominant mechanisms regulated by superfluidity. If both n and p superfluidities are relatively strong (upper right corners of

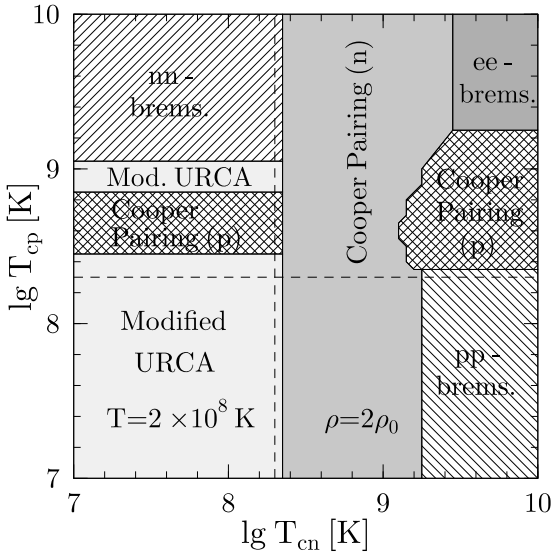

Fig. 3. Domains of the neutron and proton critical temperatures T_{cn} and T_{cp} in which different neutrino emission mechanisms dominate in a NS core at $\rho = 2\,\rho_0$ and $T = 2 \times 10^8$ K. Dashes show the lines of $T = T_{cn}$ and $T = T_{cp}$.

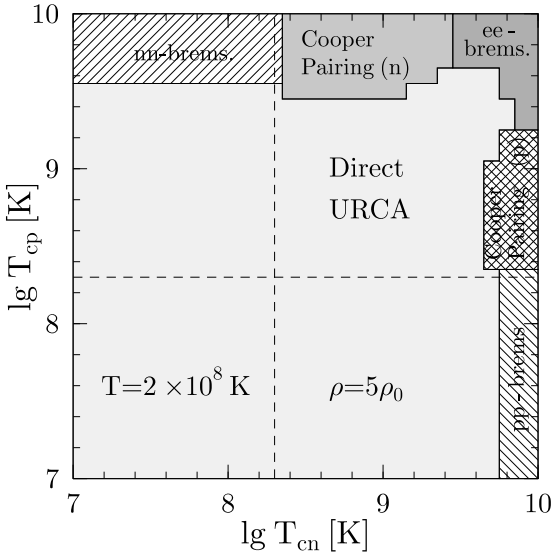

Fig. 4. Same as in Fig. 3 but for the neutrino emission enhanced by the direct Urca process at $\rho = 5\,\rho_0$.

Figs. 3 and 4), they switch off all the neutrino emission mechanisms involving nucleons, and therefore, the neutrino emission due to *ee* bremsstrahlung dominates. This region becomes wider with decreasing temperature T (*e.g.*, during NS cooling). Therefore, one of two reactions considered in this article, neutrino *ee* bremsstrahlung, can be the dominant neutrino reaction in both cases of standard and enhanced cooling. We will not discuss all variety of mechanisms which may dominate at different T_{cn}, T_{cp} and T but notice that all of them are easily implemented into the cooling codes since their emissivities are described by simple fitting formulae [3, 7, 11, 12, 21]. The present article supplements this description with new neutrino reactions.

7. Conclusions

We have analyzed two neutrino emission mechanisms in the cores of neutron stars: neutrino *ee* and *ep* bremsstrahlung. We have obtained simple expressions for calculating the neutrino energy emission rates in these reactions (Sects. 4 and 5). We have shown (Sect. 6) that the neutrino *ee* bremsstrahlung can dominate in superfluid cores of NSs in some domains of parameters of neutron-star matter. Therefore this reaction should be included in simulations of neutron star cooling.

One may expect that *ee* bremsstrahlung will be the main neutrino production mechanism in highly superfluid cores ($T_{cn} \gtrsim 3\times10^9$ K and $T_{cp} \gtrsim 3\times 10^9$ K) of sufficiently old NSs (age $t \gtrsim 10^5$ yr) during the transition from the neutrino cooling stage to the photon cooling stage.

The authors are very grateful to D.G. Yakovlev for numerous stimulating discussions and for the assistance in the preparation of the text of the present paper. They are also grateful to Kseniya Levenfish for the assistance in preparation of Figs. 3 and 4. One of the authors (ADK) acknowledges excellent working conditions and hospitality of N. Copernicus Astronomical Center in Warsaw. This work was supported in part by the RBRF (grant No. 99-02-18099a), INTAS (grant No. 96-0542), and KBN (grant 2 P03D 014 13).

REFERENCES

[1] C.J. Pethick, *Rev. Mod. Phys.* **64**, 1133 (1992).

[2] B.L. Friman, O.V. Maxwell, *Astrophys. J.* **232**, 541 (1979).

[3] D.G. Yakovlev, K.P. Levenfish, *Astron. Astrophys.* **297**, 717 (1995).

[4] J.M. Lattimer, M. Prakash, C.J. Pethick, P. Haensel, *Phys. Rev. Lett.* **66**, 2701 (1991).

[5] T. Takatsuka, R. Tamagaki, *Progr. Theor. Phys. Suppl.* **112**, 27 (1993).

[6] T. Takatsuka, R. Tamagaki, *Progr. Theor. Phys.* **97**, 345 (1997).

[7] K.P. Levenfish, D.G. Yakovlev, *Astron. Lett.* **22**, 47 (1996).

[8] E. Flowers, M. Ruderman, P. Sutherland, *Astrophys. J.* **205**, 541 (1976).

[9] D. Voskresensky, A. Senatorov, *Sov. Phys. JETP* **63**, 885 (1986).

[10] D. Voskresensky, A. Senatorov, *Sov. J. Nucl. Phys.* **45**, 411 (1987).

[11] D.G. Yakovlev, A.D. Kaminker, K.P. Levenfish, in *Neutron Stars and Pulsars*, N. Shibazaki, N. Kawai, S. Shibata, T. Kifune (eds.), Universal Academy Press, Tokyo 1998, p. 195.

[12] D.G. Yakovlev, A.D. Kaminker, K.P. Levenfish, *Astron. Astrophys.* **343**, 650 (1999).

[13] A.D. Kaminker, P. Haensel, D.G. Yakovlev, submitted to *Astron. Astrophys.* (1999).

[14] C. Schaab, F. Weber, M.K. Weigel, N.K. Glendenning, *Nucl. Phys.* **A605**, 531 (1996).

[15] A.D. Kaminker, D.G. Yakovlev, P. Haensel, *Astron. Astrophys.* **325**, 391 (1997).

[16] P. Cazzola, A. Saggion, *Nuovo Cimento* **A63**, 354 (1969).

[17] P. Cazzola, A. Saggion, *Nuovo Cimento* **A63**, 367 (1969).

[18] C.P. Lorenz, D.G. Ravenhall, C.J. Pethick, *Phys. Rev. Lett.* **70**, 379 (1993).

[19] E.M. Lifshitz, L.P. Pitaevskii, *Statistical Physics*, part 2, Pergamon, Oxford 1980.

[20] O.Y. Gnedin, D.G. Yakovlev, *Nucl. Phys.* **A582**, 697 (1995).

[21] K.P. Levenfish, D.G. Yakovlev, *Astron. Lett.* **20**, 43 (1994).

[22] V.B. Berestetskii, E.M. Lifshitz, L.P. Pitaevskii, *Quantum Electrodynamics*, Pergamon, Oxford 1982.

[23] G.G. Festa, M.A. Ruderman, *Phys. Rev.* **180**, 1227 (1969).

[24] P. Haensel, A.D. Kaminker, D.G. Yakovlev, *Astron. Astrophys.* **314**, 328 (1996).

[25] D.G. Yakovlev, V.A. Urpin, *Sov. Astron.* **24**, 303 (1980).

[26] P. Haensel, V.A. Urpin, D.G. Yakovlev, *Astron. Astrophys.* **229**, 133 (1990).

[27] M. Prakash, T.L. Ainsworth, J.M. Lattimer, *Phys. Rev. Lett.* **61**, 2518 (1988).

[28] D. Page, J.H. Applegate, *Astrophys. J.* **394**, L17 (1992).

[29] R. Tamagaki, *Progr. Theor. Phys.* **44**, 905 (1970).

[30] L. Amundsen, E. Østgaard, *Nucl. Phys.* **A442**, 163 (1985).

[31] Ø. Elgarøy, L. Engvik, M. Hiorth-Jensen, E. Osnes, *Nucl. Phys.* **A604**, 466 (1996).

[32] J. Wambach, T.L. Ainsworth, D. Pines, *Nucl. Phys.* **A555**, 128 (1993).